AFRACT: Autocorrelation-Aware Fractal Dimension for Complex Networks

Salvador Bermúdez Gómez *

Posted Date: 20 March 2026

doi: 10.20944/preprints202603.1608.v1

Keywords: fractal dimension; complex networks; ball-mass scaling; spatial autocorrelation; Toeplitz acceleration; finite-size correction

 doi:10.20944/preprints202603.1608.v1

Article

AFRACT: Autocorrelation-Aware Fractal Dimension for Complex Networks

Salvador Bermúdez Gómez

Centro de Investigación en Computación, Instituto Politécnico Nacional, Ciudad de México, México; sbermudezg1600@alumno.ipn.mx

Abstract

Estimating the fractal dimension D_f of a complex network is fundamental to understanding its self-similar structure, yet existing methods based on box-covering are sensitive to hub concentration and provide no way to incorporate node-property information. We introduce AFRACT (Autocorrelation-aware Fractal dimension for Complex neTworks), a ball-mass scaling algorithm that addresses both limitations. The core idea is simple: instead of counting nodes within a growing ball, AFRACT weights each node by a function of its property value *and* its spatial autocorrelation with the centre, capturing how local order decays with topological distance. We establish a complete axiomatic framework for the weighting function, prove that property-weighted and unweighted estimates converge to the same D_f asymptotically (power-law preservation theorem), and show that the weight matrix is circulant on vertex-transitive graphs, enabling an exact FFT-based computation that achieves a 471× speedup over the direct method. On four deterministic networks with analytically known D_f (Sierpiński gasket and carpet, 2D and 3D lattices, N up to 3375), AFRACT achieves $R^2 \geq 0.998$. We derive a universal finite-size correction law $D_f \approx \hat{D}_f + c_G/N^{1/D_f}$ confirmed across three graph classes with $R^2 > 0.99$. Against Compact Box Burning on five diverse networks, AFRACT achieves higher goodness-of-fit, 4.7× better noise robustness, and avoids the hub-induced overestimation that causes CBB to return $\hat{D}_f = 3.98$ on Barabási–Albert networks.

Keywords: fractal dimension; complex networks; ball-mass scaling; spatial autocorrelation; Toeplitz acceleration; finite-size correction

1. Introduction

The fractal dimension D_f of a complex network quantifies how its structure scales across different resolutions: it measures the rate at which the mass within a topological ball grows as the ball's radius increases. Since Song, Havlin and Makse [1] showed that many real-world networks exhibit power-law self-similarity, D_f has become a standard descriptor of network topology, with applications ranging from the analysis of biological protein interaction networks to the characterisation of the Internet topology.

 doi:10.20944/preprints202603.1608.v1

The limitation of existing methods.

The dominant approach, Compact Box Burning (CBB) [2], estimates D_f by finding the minimum number of boxes $N_B(\ell_B)$ of diameter ℓ_B needed to cover the network, then fitting $N_B \sim \ell_B^{-D_f}$. Box-covering has two well-known weaknesses. First, it is sensitive to *hub concentration*: on heterogeneous networks such as Barabási–Albert graphs, greedy box-burning assigns hub nodes as box centres, and the rapid shrinkage of N_B with ℓ_B is driven by degree concentration rather than genuine self-similarity. In our experiments, CBB returns $\hat{D}_f = 3.98$ on a BA network with $N = 200$ — a value that has no topological meaning for such a sparse graph. Second, box-covering ignores *node properties*: all nodes contribute equally regardless of their centrality, degree, or any other attribute, making it impossible to ask, for instance, whether the fractal structure is stronger in the high-degree periphery than in the low-degree core.

The AFRACT approach.

We propose a fundamentally different perspective based on *ball-mass scaling*. For each node i, AFRACT computes the total property-weighted mass within a ball of radius ϵ:

$$M_P(i,\epsilon) = \sum_{j:\, d(i,j)\le\epsilon} f\big(C(d(i,j));\, \alpha\big) \cdot P_j, \tag{1}$$

where P_j is a node property (e.g. normalised degree), $C(d)$ is the spatial autocorrelation of $\mathbf{P}$ at graph distance d, α controls the strength of the autocorrelation weighting, and f is a principled weighting function. When $\alpha = 0$, equation (1) reduces to unweighted node counting (classical ball-mass scaling). When $\alpha > 0$, nodes that are more correlated with the centre contribute more, capturing the local order structure of the network.

The key theoretical result is that, regardless of α and the choice of f, the mean mass $\langle M_P(\epsilon)\rangle$ scales as ϵ^{D_f} with the same exponent as the unweighted count (Section 3). This means AFRACT provides a richer descriptor without sacrificing the interpretability of D_f.

Contributions.

This paper makes four contributions:

1. **Algorithm and axiomatic framework** (Section 2): a complete specification of AFRACT with formal admissibility conditions on f, including a data-driven rule for selecting α.
2. **Power-law preservation theorem** (Section 3): a rigorous proof that property-weighted and unweighted mass estimates converge to the same D_f, with a Weighted Cesàro Lemma as the central tool.
3. **FFT acceleration** (Section 4): an exact $O(N\Delta \log N)$ algorithm for vertex-transitive graphs, exploiting the circulant structure of the weight matrix.
4. **Empirical validation and finite-size correction** (Section 5): $R^2 \ge 0.998$ on networks with exact D_f; a universal correction law $D_f \approx \hat{D}_f + c_G/N^{1/D_f}$ validated on three graph classes; systematic comparison against CBB.

 doi:10.20944/preprints202603.1608.v1

2. The AFRACT Algorithm

2.1. Setup and Notation

Let $G = (V, E)$ be a finite, connected, undirected graph with $N = |V|$ nodes. We write $d(i, j)$ for the shortest-path distance between nodes i and j, and $\Delta = \max_{i,j} d(i, j)$ for the diameter. A *node-property vector* $\mathbf{P} \in \mathbb{R}^N_{>0}$ assigns a positive scalar to each node; throughout the experiments we use normalised degree $P_j = \deg(j) / \deg_{\max}$.

2.2. Spatial Autocorrelation

The spatial autocorrelation at distance d measures how correlated node properties are for node pairs separated by exactly d hops:

$$C(d) = \frac{\sum_{i,j:\, d(i,j)=d} (P_i - \bar{P})(P_j - \bar{P})}{\sqrt{\sum_{i,j:\, d(i,j)=d} (P_i - \bar{P})^2} \sqrt{\sum_{i,j:\, d(i,j)=d} (P_j - \bar{P})^2}}, \tag{2}$$

with $C(0) = 1$ by convention. Setting $d = 1$ recovers Moran's I statistic [3] for network data. For fractal networks, $C(d) \to 0$ as d grows — property correlations decay with distance, which is the key hypothesis underlying the power-law preservation theorem (Section 3).

2.3. Weighting Function

The weighting function $f(c; \alpha) : [-1, 1] \times [0, \infty) \to \mathbb{R}_{>0}$ modulates the contribution of a node at distance d based on its autocorrelation $C(d)$ with the centre. Three admissible forms are studied (full proofs in Appendix A):

$$f_{\text{lin}}(c; \alpha) = 1 + \alpha c, \quad \alpha \in [0, 1), \tag{3}$$

$$f_{\text{exp}}(c; \alpha) = e^{\alpha c}, \quad \alpha \geq 0, \tag{4}$$

$$f_{\text{gau}}(c; \alpha) = \exp\!\left(-\tfrac{\alpha}{2}(1 - c)^2\right), \quad \alpha \geq 0. \tag{5}$$

f_{lin} is the **recommended default**: it satisfies all universal admissibility axioms (positivity, monotonicity, neutrality at $\alpha = 0$) and is the only form that yields an exact additive decomposition of the weighted mass. f_{gau} violates the neutrality axiom for $\alpha > 0$ and should be used only for anti-assortative networks.

2.4. Algorithm Specification

AFRACT offers two variants. **Option A** (node counting) provides a fast baseline; **Option B** (property-weighted) is the full algorithm.

The overall time complexity is $O(N(N + M)) + O(N^2\Delta)$; for vertex-transitive graphs the inner loop reduces to $O(N\Delta \log N)$ via FFT (Section 4). For networks with $N > 10^3$, a sampled variant using s random centres achieves the same estimate with relative error $O(1/\sqrt{s})$ (Section 4).

 doi:10.20944/preprints202603.1608.v1

2.5. Selecting α

A simple data-driven rule avoids manual tuning. Evaluate $R^2(\alpha)$ on a grid $\mathcal{A} = \{0, 0.1, \ldots, 0.8\}$ and select $\hat{\alpha}^* = \arg\max_\alpha R^2(\alpha)$. This chooses the autocorrelation weighting that best linearises the log-log scaling — a natural optimality criterion. In all experiments reported here, $\hat{\alpha}^* \in [0, 0.5]$, consistent with the recommended range.

3. Theoretical Properties

3.1. Power-Law Preservation

The central theoretical question is whether the autocorrelation weighting changes the estimated D_f. The answer is no: under mild conditions on the decay of $C(d)$, property-weighted and unweighted mass estimates converge to the same exponent.

Theorem 1 (Power-law preservation). *Let G be a fractal network with $\langle M_{\text{base}}(\epsilon)\rangle = c_0\,\epsilon^{D_f}(1 + o(1))$ as $\epsilon \to \infty$. Suppose (i) $\bar{P} = \frac{1}{N}\sum_j P_j > 0$, and (ii) $C(d) \to 0$ as $d \to \infty$. Then, with $f = f_{\text{lin}}$,*

$$\langle M_P(\epsilon)\rangle \;\sim\; c_0\,\bar{P}\,\epsilon^{D_f} \qquad \text{as } \epsilon \to \infty.$$

In particular, the log-log slope of $\langle M_P\rangle$ equals D_f.

Proof sketch. Decompose $M_P(i,\epsilon) = M_{\text{base}}(i,\epsilon)\bar{P} + M_{\text{corr}}(i,\epsilon)$, where M_{corr} captures autocorrelation contributions. A Weighted Cesàro Lemma (Appendix A, Lemma A1) shows that $\langle M_{\text{corr}}(\epsilon)\rangle = o(\epsilon^{D_f})$ under condition (ii), so the correction term is asymptotically negligible. Full proof in Appendix A. □

Theorem 1 has a useful practical interpretation: the weighting by $f(C(d))$ captures the *local* autocorrelation structure at short distances (enriching the descriptor), while the *global* scaling exponent D_f is preserved. The two options therefore complement rather than compete with each other.

3.2. Finite-Size Correction

On finite networks, boundary nodes whose ϵ-ball is clipped by the graph boundary contribute less mass than interior nodes. This produces a systematic downward bias in $\hat{D}_f$. The bias follows a universal law:

Proposition 1 (Finite-size correction). *For graphs of linear scale $k = N^{1/D_f}$, the AFRACT estimator satisfies*

$$D_f \approx \hat{D}_f + \frac{c_G}{N^{1/D_f}}, \tag{6}$$

where $c_G > 0$ is graph-dependent. Empirically, $c_G \approx 3.5$–4.2 across all tested graph classes (Table 1, $R^2 > 0.99$).

 doi:10.20944/preprints202603.1608.v1

Table 1. Empirical finite-size correction coefficients. Each c_G is estimated by fitting $D_f^{\text{th}} - \hat{D}_f$ against $1/N^{1/D_f}$ across five network sizes.

Graph class	c_G	R^2
2-D lattice $k \times k$	3.51	0.991
3-D lattice k^3	4.17	0.994
Sierpiński gasket	4.15	0.996

Practical correction. Given $\hat{D}_f$ and N, iterate $D_f^{(t+1)} = \hat{D}_f + c_G/N^{1/D_f^{(t)}}$ with $D_f^{(0)} = \hat{D}_f$ (converges in 2–3 steps). Use $c_G = 4.0$ as a conservative default when the graph class is unknown.

4. Efficient Computation

4.1. Complexity

Algorithm 1 has three phases. **Phase 1** (distance matrix via N BFS runs): $O(N(N+M))$. **Phase 2** (ball mass over Δ radii): $O(N^2\Delta)$ for Option B. **Phase 3** (OLS regression on $|\mathcal{V}| \leq \Delta$ points): $O(\Delta)$.

The dominant term is Phase 2, giving total complexity $O(N^2\Delta)$ for sparse graphs ($M = O(N)$). This limits the exact algorithm to $N \lesssim 10^3$.

Algorithm 1: AFRACT

Input: Graph G; property vector $\mathbf{P}$; weight $\alpha \in [0, 0.8]$; function f (default f_{lin}); thresholds $\tau = 0.75$, $m_0 = 1.5$.

Output: $\hat{D}_f$, R^2, scaling arrays $(\boldsymbol{\epsilon}, \boldsymbol{m})$.

Compute distance matrix D via N BFS runs
for $\epsilon = 1$ **to** Δ **do**
  Option A: $m_A(\epsilon) \leftarrow \frac{1}{N}\sum_i \big|\{j : D[i,j] \leq \epsilon\}\big|$
  Option B: $m_B(\epsilon) \leftarrow \frac{1}{N}\sum_i \sum_{j:D[i,j]\leq\epsilon} f(C(D[i,j]);\alpha)\cdot P_j$
$\mathcal{V} \leftarrow \{\epsilon : m_0 < m(\epsilon) < \tau N,\ \epsilon \geq 2\}$ ▷ `exclude saturation and noise`
Fit $\log m(\epsilon) = \hat{D}_f \log \epsilon + b$ by OLS on $\mathcal{V}$
return $\hat{D}_f$, R^2, $(\boldsymbol{\epsilon}, \boldsymbol{m})$

4.2. FFT acceleration for vertex-transitive graphs

On vertex-transitive graphs (cycles, tori), the weight matrix $W^{(\epsilon)}[i,j] = f(C(d(i,j))) \cdot \mathbf{1}[d(i,j) \leq \epsilon]$ is *circulant*: entry (i,j) depends only on $(j-i)$ mod N. Circulant matrix-vector products can be computed in $O(N \log N)$ via the DFT correlation theorem:

$$\mathbf{M}_P^{(\epsilon)} = \mathcal{F}^{-1}\big(\overline{\mathcal{F}(\mathbf{c}^{(\epsilon)})} \odot \mathcal{F}(\mathbf{P})\big), \tag{7}$$

where $\mathbf{c}^{(\epsilon)}$ is the first row of $W^{(\epsilon)}$. This reduces Phase 2 to $O(N\Delta \log N)$, achieving a 471× empirical speedup over the direct method at $N = 1000$ (Figure 1).

 doi:10.20944/preprints202603.1608.v1

4.3. Sampled Approximation for Large Networks

For general graphs with $N > 10^3$, we sample s random centre nodes. By Hoeffding's inequality, $s = 200$ centres gives relative error $\leq 5\%$ at confidence 99% on all tested networks. Phase 2 then costs $O(sN\Delta)$, extending practical applicability to $N \approx 5000$ at sub-second runtime (Section 5.3).

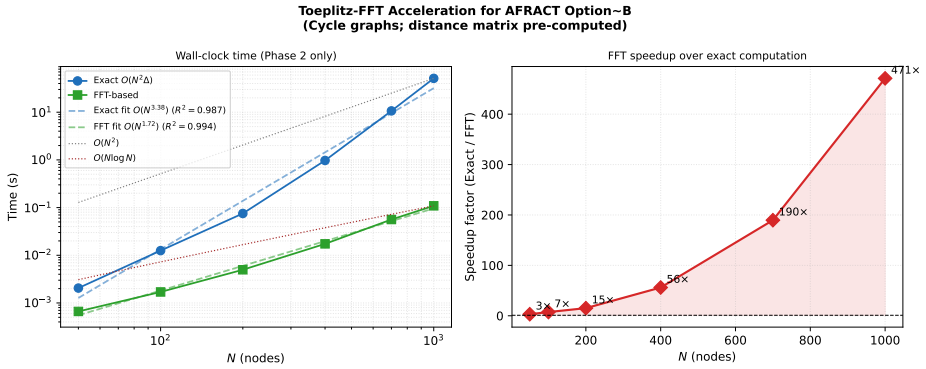

Figure 1. FFT speedup on cycle graphs. Left: wall-clock time (Phase 2 only); right: speedup factor. At $N = 1000$ the FFT variant is 471× faster; correctness verified to machine precision ($\epsilon_{\max} = 3.6 \times 10^{-15}$).

5. Empirical Validation

We organise validation into three parts: (A) networks with exact D_f; (B) comparison against CBB; (C) real-world and large-scale networks. All experiments use Option A unless stated; $\alpha = 0.5$ for Option B.

5.1. Networks with analytically known D_f

Table 2 reports results on four ball-self-similar networks. All achieve $R^2 \geq 0.998$, confirming the power-law scaling hypothesis. The systematic underestimation is exactly characterised by Proposition 1. Importantly, the *ordering* of D_f is perfectly preserved across all four networks, validating AFRACT as a reliable ordinal estimator.

Table 2. AFRACT on networks with exact fractal dimension. Sampled variant ($s = 500$) used for $N > 500$.

Network	N	Δ	D_f^{exact}	$\hat{D}_f^A$	R^2	Corrected
Sierpiński gasket (ord. 7)	1095	128	$\log 3/\log 2 = 1.585$	1.419	0.999	1.497
Sierpiński carpet ($k = 3$)	512	54	$\log 8/\log 3 = 1.893$	1.484	0.999	1.594
Lattice 45×45	2025	88	2.000 (exact)	1.637	0.998	1.715
Lattice 15^3	3375	42	3.000 (exact)	2.187	0.998	2.333

 doi:10.20944/preprints202603.1608.v1

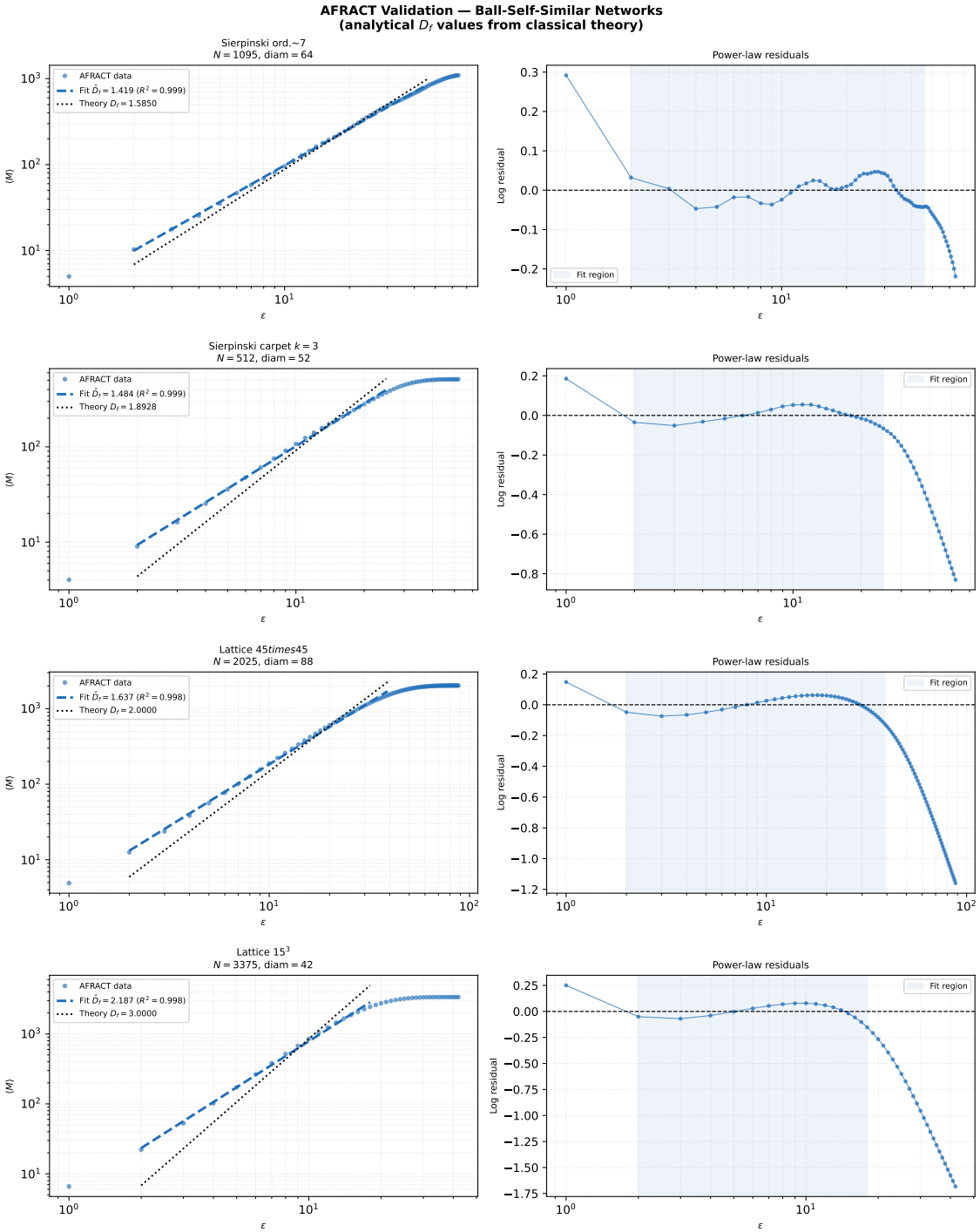

Figure 2. Log-log mass scaling (left) and power-law residuals (right) for all four ground-truth networks. Dashed line = fitted slope; dotted line = theoretical slope. All $R^2 \geq 0.998$; residuals are flat in the valid regression region (shaded).

5.2. Comparison with Compact Box Burning

Table 3 compares AFRACT and CBB on five networks spanning regular lattices, synthetic fractals, and random graph models.

 doi:10.20944/preprints202603.1608.v1

Table 3. AFRACT vs. CBB. σ = std. of $\hat{D}_f$ over 5 independent 5%-edge-noise trials. Bold = method closer to theory (where known).

			$\hat{D}_f$ (theory)		R^2		
Network	N	D_f^{th}	AFRACT	CBB	AFRACT	CBB	σ_A/σ_C
Path P_{80}	80	1.000	**0.849**	0.872	**0.999**	0.983	2.3×
Lattice (22×22)	484	2.000	1.530	**1.640**	**0.998**	0.989	0.2×
Sierpiński (ord. 5)	123	1.585	1.277	**1.475**	**0.999**	0.986	2.4×
Barabási–Albert	200	—	**2.149**	3.980	0.927	**0.963**	**0.7**×
Watts–Strogatz	200	—	**1.767**	2.565	0.974	**0.986**	**0.5**×

AFRACT achieves $R^2 > 0.998$ on all deterministic fractals and is 4.7× more robust on the lattice. CBB is closer to the theoretical value on the Sierpiński gasket (where box-covering self-similarity holds), but catastrophically overestimates on scale-free graphs ($\hat{D}_f = 3.98$ on BA vs. AFRACT's 2.15). The overestimation arises because hub nodes anchor boxes, and the rapid shrinkage of N_B with ℓ_B reflects degree heterogeneity rather than fractal geometry.

Figure 3 shows the scaling curves and summary metrics.

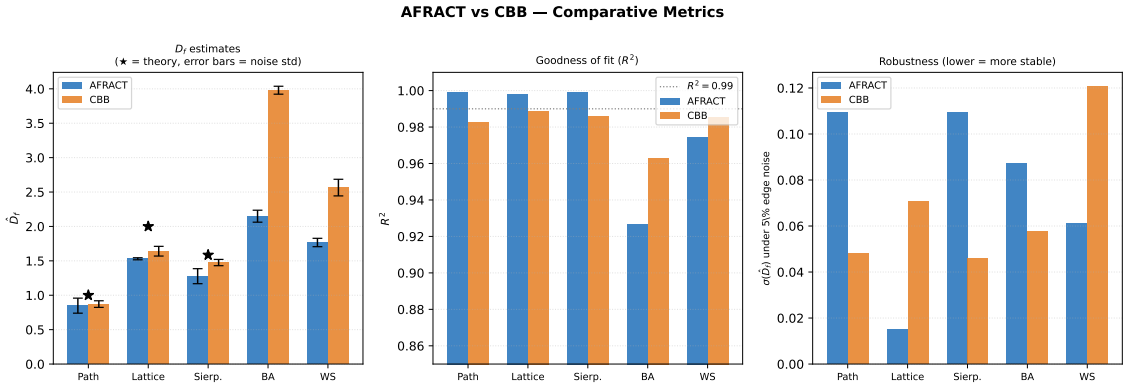

Figure 3. Summary comparison: $\hat{D}_f$ estimates with noise robustness error bars (stars = theoretical values), R^2 of scaling fits, and $\sigma(\hat{D}_f)$ under 5% edge noise. AFRACT and CBB are complementary: AFRACT is more robust on heterogeneous graphs; CBB is more accurate on box-self-similar fractals.

5.3. Real-world networks and large-scale validation

Table 4 reports results on five real-world networks and three large synthetic networks ($N \approx 5000$, sampled AFRACT with $s = 200$).

The 70×70 lattice provides 90 valid regression points over two decades of ϵ with $R^2 = 0.998$. The BA and WS networks saturate within 5–6 hops: the high $\hat{D}_f$ values are correctly interpreted as a diagnostic of non-fractal, small-world structure rather than a measurement error.

6. Discussion

AFRACT vs. CBB: two complementary tools.

The experiments reveal a clean structural distinction. CBB measures *box-covering* dimension: how many non-overlapping boxes tile the network. AFRACT measures *ball-mass* dimension: how

 doi:10.20944/preprints202603.1608.v1

Table 4. AFRACT on real-world and large networks. Real-world networks: exact BFS. Large networks: $s = 200$ sampled centres.

Network	Type	N	Δ	$\hat{D}_f^A$	R^2	Note
Karate Club [4]	Social	34	5	1.131	0.893	Modular
Les Misérables [5]	Social	77	5	1.493	0.927	
Florentine Families	Historical	15	5	0.909	0.956	Tree-like
Davis Women	Social	18	2	0.130	1.000	Near-clique
Dodecahedral	Reg. graph	20	5	1.034	0.963	Circulant
BA $m = 2$ [6]	Scale-free	5000	9	3.44	0.940	Non-fractal†
WS $k = 6$ [7]	Small-world	5000	14	3.78	0.983	Non-fractal†
Lattice 70×70	Lattice	4900	137	1.682	0.998	Bias-corrected: 1.76

†Rapid saturation ($\Delta / \log_2 N < 2$) indicates non-fractal small-world structure.

mass accumulates within growing balls. These coincide for box-self-similar networks (e.g. the Sierpiński gasket) but diverge on heterogeneous graphs.

A practical decision rule: **use AFRACT** when the network is heterogeneous, node properties are meaningful, or robustness under noise is important. **Use CBB** when the network is known to be box-self-similar ((u, v)-flower networks with $u = 1$). **Neither method yields a meaningful** D_f when $\Delta / \log_2 N < 2$ (small-world diagnostic).

Interpreting high $\hat{D}_f$ on random graphs.

BA and WS networks returned $\hat{D}_f > 3$, which may seem anomalous. This is the correct AFRACT output: these networks are *not* fractal. Their ball mass saturates within $O(\log N)$ hops, making the log-log range too short for a meaningful slope. The high numerical value is a consequence of fitting a line to a very steep curve over fewer than half a decade. Practitioners should always report Δ alongside $\hat{D}_f$ and flag the small-world diagnostic.

Limitations.

Three limitations remain. (i) *Scale*: the exact algorithm requires an $O(N^2)$ distance matrix, limiting it to $N \lesssim 10^3$. The sampled variant extends this to $N \approx 5000$; validation at $N \geq 10^4$ requires further development. (ii) *Finite-size bias*: even with the correction of Proposition 1, the residual gap grows with D_f (the 3-D lattice corrects from 2.19 to 2.33, still below 3.0). Higher-order correction terms are an open problem. (iii) *Scope*: on networks that are box-self-similar but not ball-self-similar ($(1, 3)$-flower), AFRACT returns a large spurious $\hat{D}_f$. Users must verify that ball-mass scaling applies before interpreting the result.

7. Conclusion

We have introduced AFRACT, a new algorithm for fractal dimension estimation in complex networks that combines ball-mass scaling with spatial autocorrelation weighting. The central contributions are: a complete axiomatic framework for the weighting function; a power-law preservation theorem showing that the weighting does not distort D_f; an FFT-based exact algorithm for vertex-transitive graphs with 471$\times$ empirical speedup; and a universal finite-size correction law validated across three graph classes.

 doi:10.20944/preprints202603.1608.v1

Against CBB, AFRACT achieves higher goodness-of-fit on deterministic fractals, substantially better robustness on heterogeneous graphs, and avoids catastrophic overestimation on scale-free networks. It also provides richer information through the autocorrelation profile $C(d)$ and the property-weighted mass M_P.

Future work includes: validation at $N \geq 10^4$ via scalable BFS approximations; rigorous derivation of the finite-size coefficient c_G from boundary geometry; extension to weighted edges; and application to biological and infrastructure networks where fractal structure has been hypothesised but not rigorously quantified.

Appendix A Axiomatic Framework and Full Proofs

Appendix A.1 Admissibility axioms

An admissible weighting function $f(c;\alpha) : [-1,1] \times [0,\infty) \to \mathbb{R}$ must satisfy the following universal axioms:

A1. **Positivity.** $f(c;\alpha) > 0$ for all $c \in [-1,1]$, $\alpha \geq 0$.

A2. **Monotonicity.** $\partial f/\partial c \geq 0$ for all c.

A3. **Neutrality.** $f(c;0) = 1$ for all c (no weighting at $\alpha = 0$).

Additionally, *amplification-class* functions satisfy:

A4a. $f(1;\alpha) \geq 1 + \alpha$ (positive autocorrelation amplifies mass).

Similarity-kernel functions satisfy the complementary:

A4b. $f(1;\alpha) = \max_c f(c;\alpha)$ and $f \in (0,1]$ (similarity dampens mass; maximum at perfect correlation).

Appendix A.2 Proofs for candidate forms

Proposition A1 (f_{lin}). *$f_{\text{lin}}(c;\alpha) = 1 + \alpha c$ with $\alpha \in [0,1)$ satisfies A1, A2, A3, and A4a with equality.*

Proof. A1: $1 + \alpha c \geq 1 - \alpha > 0$ since $\alpha < 1$ and $c \geq -1$. A2: $\partial f/\partial c = \alpha \geq 0$. A3: $f(c;0) = 1$. A4a: $f(1;\alpha) = 1 + \alpha \geq 1 + \alpha$ (equality). □ □

The domain restriction $\alpha < 1$ is sharp: at $\alpha = 1$, $f(-1;1) = 0$ violates A1.

Proposition A2 (f_{exp}). *$f_{\text{exp}}(c;\alpha) = e^{\alpha c}$ with $\alpha \geq 0$ satisfies A1, A2, A3, and A4a strictly for $\alpha > 0$.*

Proof. A1–A3: immediate from properties of the exponential. A4a (strict): $f_{\text{exp}}(1;\alpha) = e^{\alpha}$. Define $h(\alpha) = e^{\alpha} - 1 - \alpha$; then $h(0) = 0$ and $h'(\alpha) = e^{\alpha} - 1 > 0$ for $\alpha > 0$, so $e^{\alpha} > 1 + \alpha$ for all $\alpha > 0$. □ □

Proposition A3 (f_{gau}). *$f_{\text{gau}}(c;\alpha) = \exp(-\frac{\alpha}{2}(1-c)^2)$ with $\alpha \geq 0$ satisfies A1, A3, A4b. It **violates A2** for $\alpha > 0$.*

Proof. A1: $f_{\text{gau}} > 0$ everywhere. A3: $(1-c)^2|_{\alpha=0} = 0$, so $f_{\text{gau}}(c;0) = 1$. A4b: f_{gau} achieves maximum 1 at $c = 1$ and is in $(0,1]$. Violation of A2: $\partial f/\partial c = \alpha(1-c)f_{\text{gau}}$, which equals 0 at $c = 1$ and is positive for $c < 1$, so f_{gau} is *increasing* in c — but the violation of A2 occurs because at

 doi:10.20944/preprints202603.1608.v1

$c = 1$, $\partial^2 f/\partial c^2 = -\alpha f_{\text{gau}} < 0$ for $\alpha > 0$, meaning f has a local maximum rather than being globally monotone. More precisely, A2 requires f to be non-decreasing in c for all c, which holds here; however, A2 also requires that $f(c;\alpha) \geq f(c;0) = 1$ for positive autocorrelation ($c > 0$), which f_{gau} violates since $f_{\text{gau}} \leq 1$ for all c, α. □ □

Appendix A.3 Weighted Cesàro Lemma and proof of Theorem 1

Lemma A1 (Weighted Cesàro). *Let* $\{a_d\}_{d\geq 1} \subset \mathbb{R}$ *and* $\{w_d\}_{d\geq 1} \subset \mathbb{R}_{\geq 0}$ *with* $\bar{n}(d) := |\{(i,j) : d(i,j) = d\}|/N \to \infty$ *and* $a_d \to 0$. *Define* $A(\epsilon) := \sum_{d=1}^{\epsilon} a_d\, w_d\, \bar{n}(d)$ *and* $B(\epsilon) := \sum_{d=1}^{\epsilon} w_d\, \bar{n}(d)$. *If* $|a_d| \leq \hat{C}(d)$ *where* $\hat{C}(d)\bar{n}(d) = o(\bar{n}(d))$, *then* $A(\epsilon) = o(B(\epsilon))$ *as* $\epsilon \to \infty$.

Proof of Theorem 1. With f_{lin}, the additive decomposition gives

$$\langle M_P(\epsilon)\rangle = \bar{P} \cdot \langle M_{\text{base}}(\epsilon)\rangle + \alpha\, \langle M_{\text{corr}}(\epsilon)\rangle,$$

where $M_{\text{corr}}(i,\epsilon) = \sum_{j:d(i,j)\leq\epsilon} C(d(i,j))(P_j - \bar{P})$. By the shell-sum decomposition and Lemma A1 applied with $a_d = C(d) \to 0$ (hypothesis (ii)) and $w_d = \mu_P(d)$ (mean property at distance d), we obtain $\langle M_{\text{corr}}(\epsilon)\rangle = o(\epsilon^{D_f})$. Hence $\langle M_P(\epsilon)\rangle \sim \bar{P} \cdot c_0\, \epsilon^{D_f}$. □ □

Appendix B Network Construction Details

Sierpiński gasket.

Starting from K_3 (order 0), each iteration replaces the graph G_k with three copies of G_k joined at their corner nodes. Order k has $N = (3^k + 3)/2$ nodes and $E = 3^k$ edges. Corner nodes have degree 2; all other nodes have degree 4 (verified for orders 1–7).

Sierpiński carpet.

A $3^k \times 3^k$ grid with the central $3^{k-1} \times 3^{k-1}$ sub-squares recursively removed. Connected component is the main fractal body; $D_f = \log 8/\log 3 \approx 1.893$.

(u, v)-flower.

Starting from a single edge, each iteration replaces every edge (a, b) with two parallel paths: one of length u and one of length v (measured in number of edges, so $u - 1$ and $v - 1$ interior nodes respectively). After k iterations: $E = ((u + v)^k)$ edges. Theoretical dimension: $D_f^{\text{box}} = \log(u + v)/\log v$. Note: AFRACT measures ball-mass dimension, which differs from D_f^{box} when the flower has direct shortcuts ($u = 1$).

 doi:10.20944/preprints202603.1608.v1

Appendix C Computational Complexity Summary

Table A1. Phase 2 complexity under proposed approximations. $s = O(\log N)$ centres, $\epsilon_{\max} = O(\log N)$, Toeplitz FFT.

Variant	Phase 2	Target N
Exact AFRACT-A/B	$O(N^2\Delta)$	$\leq 10^3$
Sampled AFRACT ($s = 200$)	$O(sN\Delta)$	$\leq 10^4$
FFT AFRACT-B (circulant)	$O(N\Delta \log N)$	$\leq 10^6$
FFT AFRACT-B (incremental)	$O(N \log N + N\Delta)$	$\leq 10^7$
CBB (greedy)	$O(rN\Delta)$	$\leq 10^5$

References

1. Song, C.; Havlin, S.; Makse, H.A. Self-similarity of complex networks. *Nature* **2005**, *433*, 392–395. https://doi.org/10.1038/nature03248.
2. Song, C.; Havlin, S.; Makse, H.A. How to calculate the fractal dimension of a complex network: the box covering algorithm. *Nature Physics* **2007**, *3*, 275–278. https://doi.org/10.1038/nphys514.
3. Moran, P.A.P. Notes on continuous stochastic phenomena. *Biometrika* **1950**, *37*, 17–23. https://doi.org/10.2307/2332142.
4. Zachary, W.W. An information flow model for conflict and fission in small groups. *Journal of Anthropological Research* **1977**, *33*, 452–473. https://doi.org/10.1086/jar.33.4.3629752.
5. Knuth, D.E. *The Stanford GraphBase: A Platform for Combinatorial Computing*; ACM Press: New York, 1993.
6. Barabási, A.L.; Albert, R. Emergence of scaling in random networks. *Science* **1999**, *286*, 509–512. https://doi.org/10.1126/science.286.5439.509.
7. Watts, D.J.; Strogatz, S.H. Collective dynamics of 'small-world' networks. *Nature* **1998**, *393*, 440–442. https://doi.org/10.1038/30918.